To cite this article: Zhou P, Fu J Y. Parameter optimization design of stern flap of displacement surface warship[J/OL]. Chinese Journal of Ship Research, 2019, 14(3). http://www.ship-research.com/CN/Y2019/V14/I3/92.
DOI:10.19693/j.issn.1673-3185. 01370

Parameter optimization design of stern flap of displacement surface warship

*Zhou Peng**, *Fu Jiangyan*
China Ship Development and Design Center, Shanghai 201108, China

Abstract: [**Objectives**] The design of stern flap usually focuses on resistance reduction at high speed. For surface warship stern flap design which is aimed at optimizing the cruise speed and design speed, the cruise speed comes in a large range, so the parameter selection of stern flap needs to be emphasized. [**Methods**] The design method combining viscous wave making flow field numerical simulation and model test verification, which take into account the navigation attitude, is used for optimization of stern flap with multiple condition parameters. Through comparative analysis on multi-option numerical simulation and resistance and self-navigation model test, the the influence of length and cathedral angle of stern flap on the resistance reduction and energy saving in the cruise speed and design speed of displacement surface warship is learned and a preliminary analytical verification of the effectiveness of CFD numerical simulation results is done. [**Results**] The results show that, by optimizing the stern flap parameters, energy consumption is reduced by 3% in cruise speed and 5% in design speed, thus the goal of energy saving in both cruise speed and maximum speed is achieved. [**Conclusions**] The research can provide theoretical support for the subsequent parametric optimization design of stern flap of displacement surface warship.

Key words: surface warship; stern flap; parametric optimization; numerical simulation; model test
CLC number: U662.2

0 Introduction

For the surface warship, the goal of resistance reduction and energy saving is always the constant pursuit. Warships have high requirements for speed, but the shortage of resources is serious and the installation of energy-saving devices is limited. As a result, the stern flap featuring convenient installation, simple structure, and good resistance-reduction effect has been gradually installed on the mainstream surface warships all over the world.

The research on the stern flap of surface warship is mainly focused on the effect of resistance reduction, the mechanism and the scale effect of model ship test all over the world. In China, Cheng and Dong et al. [1-2] revealed the mechanism of resistance reduction of stern flap for round-bilge ship and deep-V ship respectively. Cheng et al. [3-4] carried out research on the multi-scheme model tests of stern flap and the verification of real ship test for the round-bilge ship type. Zheng et al. [5] carried out multi-scheme model test of stern flap resistance reduction for the deep-V hull model. In foreign countries, since the 1990s, the US Navy has conducted a lot of experimental research on the resistance-reduction effect and the model ship scale effect of the stern flap of the Arleigh Burke class frigates [6-9] and FFG-7 class frigate [10].

It is worth noting that the design of stern flap is generally aimed at optimizing the design speed and cruise speed in the past. However, the mainstream warships all over the world have put forward higher requirements for the acoustic stealth performance in recent years. Based on the requirements of acoustic stealth and economic efficiency, medium and large surface warships in the form of combined diesel or gas propulsion will only turn on diesel units with relatively small power under the cruising conditions. Therefore, the power margin of cruising propulsion is extremely tight.

Received: 2018 - 08 - 05
Author(s): Zhou Peng, male, born in 1988, master, engineer. Research interest: overall ship research and design. E-mail: yy254114@163.com
Fu Jiangyan, female, born in 1980, Ph.D., senior engineer. Research interest: overall ship research and design
***Corresponding author**: Zhou Peng

Relevant studies show that the stern flap plays a role of resistance reduction at a certain Froude number, but if the Froude number is too low, it usually increases the resistance [5,11]. The design of stern flap parameters at high Froude number and low Froude number often produces opposite effects. All of these have put forward higher design requirements for the design of stern flap parameters of surface warships which take cruise speed and design speed as optimization goals.

In this paper, a round-bilge displacement surface warship is taken as the research object. Aiming at the optimization of cruise speed and design speed, this paper adopts CFD numerical calculation method to carry out the verification of multi-scheme resistance and self-propulsion model test, so as to optimize the design of stern flap parameters and provide guiding suggestions for the optimization of stern flap parameters of displacement surface warship.

1 Governing equation and calculation method

1.1 Governing equation and turbulence model

The flow field around the ship is a highly complex three-dimensional flow, which is mainly caused by the complicated shape of bow and stern of ship and the large change of curvature. This complex characteristic is especially reflected in the flow and wake of stern. For the accuracy of numerical calculation, the selection of turbulence model directly affects its accuracy [12-13]. In this paper, the RNG $k-\varepsilon$ turbulence model in commercial software CFX is used for simulation, and the turbulence model and governing equation [14-15] are summarized as follows.

In the rectangular coordinate system, the incompressible Newtonian fluid continuity equation and the RANS equation are

$$\frac{\partial u_i}{\partial x_i}=0 \tag{1}$$

$$\rho\frac{\partial u_i}{\partial t}+\rho u_j\frac{\partial u_i}{\partial t}=\rho F_i=\frac{\partial p}{\partial x_i}+\frac{\partial}{\partial x_j}(\mu\frac{\partial u_i}{\partial x_j}-\rho\overline{u_i'u_j'}) \tag{2}$$

where ρ is the density; μ is the viscosity coefficient of fluid; p is the average pressure; F_i is external force term; t is time; x_i and x_j are coordinate components; u_i is time average velocity; u_j is fluctuation velocity; the correlation term of fluctuation velocity $\rho\overline{u_i'u_j'}$ is called Reynolds stress.

The RNG $k-\varepsilon$ turbulence model adopted in this paper is an improved form of the standard $k-\varepsilon$ model, and the model equation is based on the renormalization of N-S equation. The model modifies the turbulent viscosity and considers the rotating and swirling flow conditions in the average flow, which is a turbulence model suitable for the calculation of ship flow field.

The kinetic energy equation of turbulence and the dissipation rate equation are

$$\frac{\partial(\rho k)}{\partial t}+\frac{\partial}{\partial x_i}(\rho u_i k)=\frac{\partial}{\partial x_j}[(\mu+\frac{\mu_t}{\sigma_k})\frac{\partial k}{\partial x_j}]+p_k-\rho\varepsilon \tag{3}$$

$$\frac{\partial(\rho\varepsilon)}{\partial t}+\frac{\partial}{\partial x_i}(\rho u_i\varepsilon)=\frac{\partial}{\partial x_j}[(\mu+\frac{\mu_t}{\sigma_\varepsilon})\frac{\partial\varepsilon}{\partial x_j}]+ C_{\varepsilon1}\frac{\varepsilon}{k}-C_{\varepsilon2}\frac{\varepsilon^2}{k}-R_\varepsilon \tag{4}$$

where k is the turbulent kinetic energy; ε is dissipation of turbulent kinetic energy; μ_t represents the viscosity coefficient of turbulence kinetic energy, $\mu_t=\rho C_\mu\frac{k^2}{\varepsilon}$; p_k is the turbulence kinetic energy generation term, $p_k=\mu_t S^2$, where $S=\sqrt{2\boldsymbol{S}_{ij}\boldsymbol{S}_{ij}}$, $\boldsymbol{S}_{ij}$ is the mean strain tensor; $\boldsymbol{S}_{ij}=\frac{1}{2}(\frac{\partial u_i}{\partial x_j}+\frac{\partial u_j}{\partial x_i})$; $R_\varepsilon=\frac{C_\mu\rho\eta^3(1-\frac{\eta}{\eta_0})}{1+\beta\eta^3}\frac{k^2}{\varepsilon}$, and $\eta=\sqrt{\frac{p_k}{\rho C_\mu\varepsilon}}$; constants σ_k = 1.39, σ_ε = 1.39, $C_{\varepsilon1}$ = 1.42, $C_{\varepsilon2}$ = 1.68, C_μ = 0.084 5, η_0 = 4.38, β = 0.012.

1.2 Adjustment equation of floating state

During the voyage, especially under a high Froude number, the change of pressure distribution will cause the imbalance of gravity and buoyancy as well as the longitudinal unbalanced torque, thus causing heave and trim.

Here, the ship can be regarded as a rigid body, and it must meet the balance of force and torque when traveling stably in still water.

$$\sum F=0 \tag{5}$$

$$\sum M_{xoz}=0 \tag{6}$$

where F is the vertical force; M_{xoz} is the longitudinal torque of external force at the center of buoyancy. Eq. (5) and Eq. (6) are considered as the equilibrium equations of floating sate.

In this paper, a simplified iterative calculation is adopted. First, it is assumed that

1) The designed water plane area remains unchanged when the ship heaves.

2) The adjustment motion of floating state is very slow.

Based on the above assumptions, the heave and trim equations are as follows.

$$F_z = mg + \rho g A w \Delta d \tag{7}$$

$$M = \Delta \overline{GM}_{\mathrm{L}} \sin\theta \tag{8}$$

where F_z is the component of pressure on the ship in the z direction (vertical); m is ship mass; g is the acceleration of gravity; Δd is the ship heave value (sink is positive); Aw is the designed water plane area; M is the component of pressure in the y direction (transverse) of the torque at the center of ship buoyancy; Δ is displacement of ship; $\overline{GM}_{\mathrm{L}}$ is the ship longitudinal stability; θ is the angle of trim of the ship (trim by stern is positive).

Based on the above assumptions, the steps to adjust the floating state in this paper are as follows.

1) The flow field and pressure distribution of the ship under the positive floating state are calculated. When the convergence state is reached, the force on the ship surface and the torque relative to the center of gravity are obtained by integrating the pressure.

2) According to the force and torque obtained in Step 1, the heave and trim of the ship are calculated for the adjustment of the attitude of the ship.

3) Under the new attitude of ship, the gird is reconstructed to solve the viscous wave-making flow field of the ship.

The above calculation steps are repeated until the balance of the force and torque in Eq. (7) and Eq. (8) is reached.

2 Calculation model

In this paper, the calculation model of a displacement round-bilge ship is established, and the relevant parameters are shown in Table 1. On the basis of sorting out a large number of literatures related to the design of the stern flap and the previous experience of the design of the stern flap parameters, the important design parameters of the stern flap are summarized as follows: stern flap length, stern flap cathedral angle, stern flap underside rake angle, and the width, thickness, outline and upper edge shape of stern flap. Based on the mechanism of resistance reduction of stern flap, the influence of stern flap parameters on ship resistance and propulsion performance is analyzed in detail, and the design parameters of stern flap which have the greatest influence on the performance of stern flap are summarized, namely the length of stern flap L and the cathedral angle of stern flap α. This paper focuses on the optimization of these two design parameters, as shown in Fig. 1.

Table 1 The main parameters of ship model

Parameter	Value
Length of ship model/m	6.57
Draught of ship model/m	0.22
Ship model displacement volume/m^3	0.55

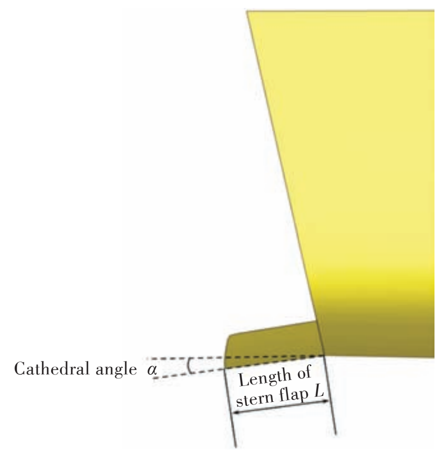

Fig.1 Schematic diagram of length and cathedral angle parameter of stern flap

In this paper, with resistance reduction at both cruise speed and design speed as the design goal, the length of stern flap and the range of its cathedral angle are determined, and more than 10 design schemes of stern flap are completed by implementing the optimal design, after we have comprehensively considered many factors such as the main dimensions, tonnage, liner characteristics of stern transom plate and navigation characteristics under the condition of no stern flap. The same scale ratio is adopted in the numerical calculation of the ship type as in the model test. The design parameters of the stern flap of the ship model are shown in Table 2.

Table 2 The cases of stern flap by numerical simulation

Case	Parameter	
	L/mm	α /(°)
A	19.2	10
B	38.5	0
C	38.5	8
D	38.5	10
E	57.7	10
F	65.4	3
G	65.4	5
H	65.4	8
I	72.1	3
J	72.1	8
K	144.2	3

By adopting the numerical calculation method based on the viscous wave-making flow field and taking into account the navigation attitude, we conducted the grid division on a total of 12 cases, including a bare-body ship model without stern flap and 11 ship models with stern flap. The surface grid division of the viscous wave-making flow field and the bow and stern of the ship model is shown in Fig. 2.

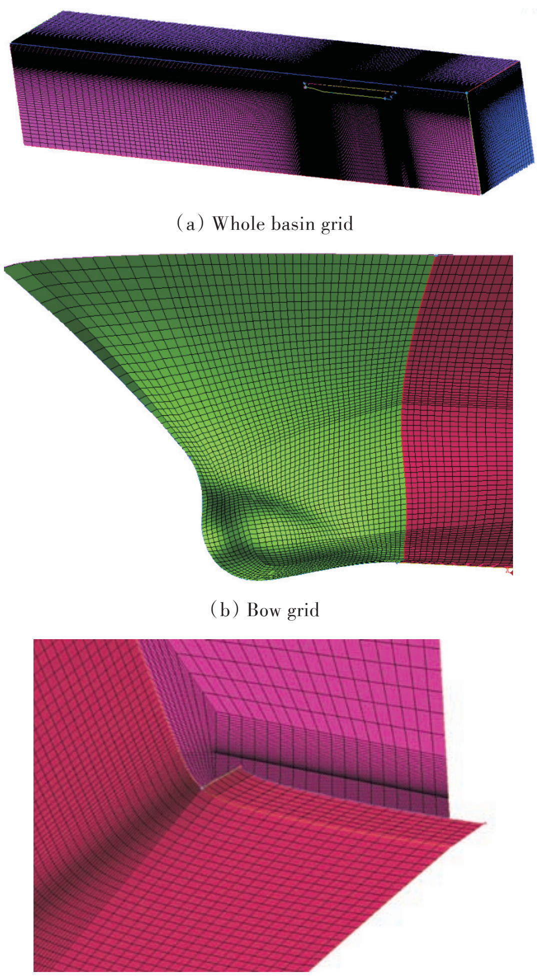

(a) Whole basin grid

(b) Bow grid

(c) Stern grid

Fig.2 Viscous wave-making flow field and bow and stern surface grid of the ship model

The grid division adopts multi-block structured grids. The grids on the ship model surface and near the waterline are properly densified, among which the number of grids in the calculation of the bare-body ship model is about 4.7 million, and the number of grids in the calculation of the bare-body ship model with stern flap is about 5 million. For the grids generated before and after the attitude adjustment of the ship model, the number and distribution of the block and grid in the fluid computation domain are the same, and all cases adopt the same numerical calculation method. Then, the comparison of multi-scheme numerical calculation is carried out.

3 Model test

The model test was carried out in the towing tank of the China Ship Scientific Research Center (CSSRC). The tank is 474 m long, 14 m wide and 7 m deep. The test ship model is made of wood, and five kinds of stern flaps are processed. The stern flap parameters are shown in Table 3. In order to verify the influence of scheme without stern flap, and scheme with stern flap and the effects of schemes with different stern flaps on the ship resistance and ship propulsion, the resistance tests are carried out on the bare-body ship model, the fully-appended ship model without stern flap and the fully-appended ship model with stern flap. Then, the self-propulsion test of the latter two ship models was carried out. The specific projects are shown in Table 4.

Table 3 The cases of stern flap for ship model test

Case	Parameter	
	L /mm	α /(°)
1	38.5	0
2	38.5	8
3	38.5	15
4	48.1	8
5	57.7	8

Table 4 The items of ship model test

Case	Resistance test	Self-propulsion test
Bare-body ship model	√	-
Fully-appended ship model without stern flap	√	√
Fully-appended ship model with stern flap(Case 1)	√	√
Fully-appended ship model with stern flap (Case 2)	√	√
Fully-appended ship model with stern flap (Case 3)	√	√
Fully-appended ship model with stern flap (Case 4)	√	√
Fully-appended ship model with stern flap (Case 5)	√	√

4 Results and analyses

4.1 Analysis of numerical calculation methods

In this paper, in order to verify the reliability of the resistance prediction method which takes into account the navigation attitude, the numerical calculation of the total resistance of the bare-body ship model under typical working conditions and the resistance decrease rate of the fully-appended model with stern flap (case 1) is compared with the model test results. The results are shown in Table 5. In the table, R_{barebody} is the total resistance of bare-body ship model; $\lambda = 1 - \dfrac{R_{\text{sternflap}}}{R}$ is the resistance decrease rate of the case with stern flap (the positive value means resistance reduction and the negative value means resistance increase), where $R_{\text{sternflap}}$ is the total resistance of the fully-appended ship model with stern flap, and R is the total resistance of the fully-appended ship model without stern flap. It should be noted that, in order to simplify the workload of numerical calculation, the stern flap optimization based on CFD numerical calculation is carried out according to the bare-body ship model. In order to verify the influence of stern flap on the propulsion efficiency of the whole ship, the comparative test on the resistance effect of stern flap is conducted based on the fully-appended ship model. In addition, the reliability of the numerical calculation can be verified by the lateral comparison of the resistance decrease ratio λ.

Table 5 The results comparison between numerical simulation and model test

Fr	R_{barebody}/N		Error/%	λ/%	
	Numerical calculation	Model test		Numerical calculation	Model test
0.25	47.8	46.2	3.4	2.3	3.1
0.42	164.8	172.8	−4.6	3.0	2.5

As can be seen from Table 5, the errors of the total bare-body resistance under the conditions of medium Froude number (Fr = 0.25) and high Froude number (Fr=0.42) are all within 5%, meeting the requirements of engineering accuracy. According to the numerical calculation and model test of Case 1, the resistance decrease rates of the two are roughly equal, which preliminarily verifies the feasibility of applying the numerical calculation method adopted in this paper to the design of stern flap resistance reduction. The conclusion is instructive.

4.2 Numerical calculation results and analysis

According to the 11 stern flap cases in Table 2 and the numerical simulation of viscous wave-making flow field, it is found that, compared with the situation without stern flap, the equipment of stern flap has a significant impact on the navigation attitude, shape of flow field behind the ship, distribution of bottom pressure field and wave shape distribution, etc. Figs. 3–5 respectively show the wave shape of ship, the stern wave height of ship and the distribution of hull surface pressure without stern flap and with stern flap B. With the change of parameters such as the stern flap length and the cathedral angle, the wake flow field with different stern flaps is obviously different. Fig. 6 shows the comparison of wave shape of wake flow with stern flap B and stern flap F under the design speed.

Numerical simulation results show that, when Fr > 0.4, the aft flow field of ship with stern flap is significantly changed. The height of wake flow decreases to

(a) Ship without stern flap

(b) Ship with stern flap B

Fig.3 Comparison of waveform of ship without stern flap and with stern flap B

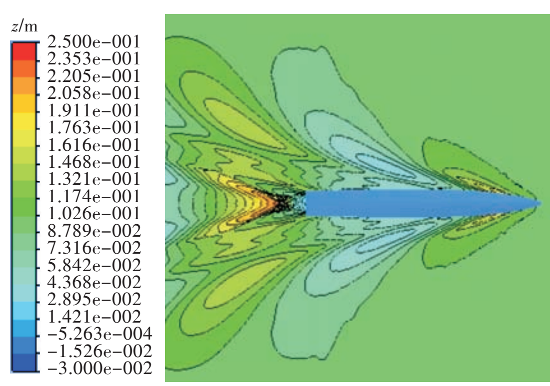

(a) Ship without stern flap

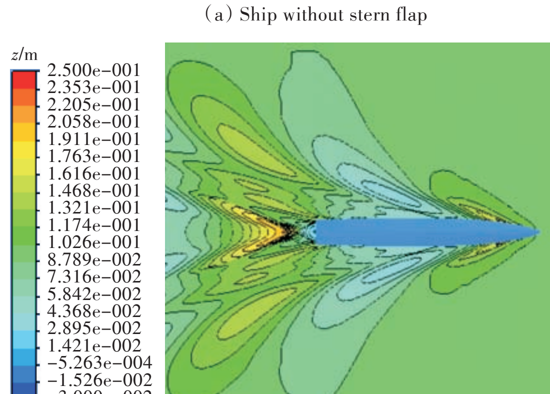

(b) Ship with stern flap B

Fig.4 Comparison of stern wave height of ship without stern flap and with stern flap B

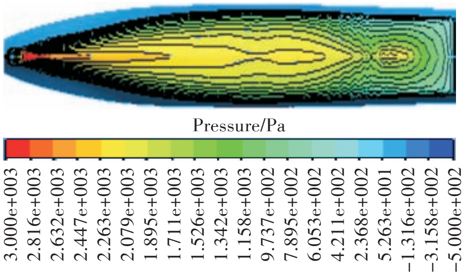

(a) Ship without stern flap

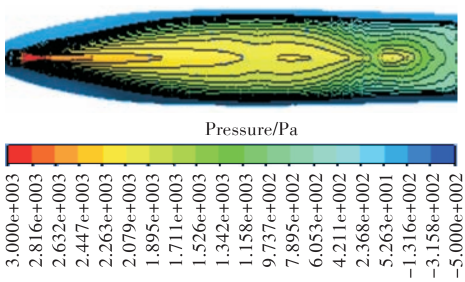

(b) Ship with stern flap B

Fig.5 Comparison of hull surface pressure distribution without stern flap and with stern flap B

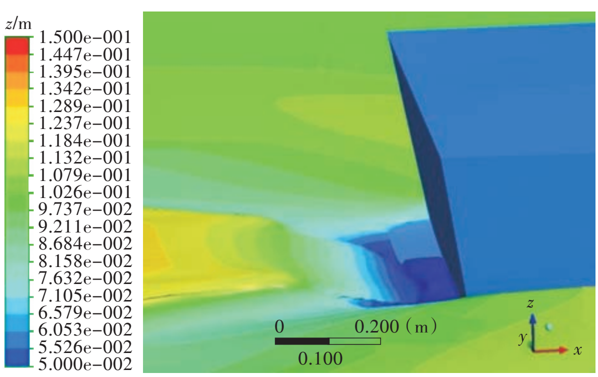

(a) Case F

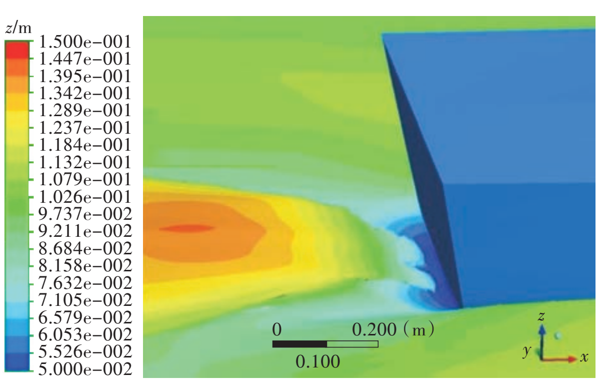

(b) Case B

Fig.6 Comparison of wave shape of wake flow for different stern flaps

some extent, and the virtual appendage is elongated. In addition, the surface pressure changes on the aft of ship are also obvious, and the aft pressure increases to some extent after installing the stern flap. Meanwhile, as the distribution of hull surface pressure changes, the navigation attitude of the ship is significantly improved, and the heave and trim of the ship with stern flap are significantly reduced at high speed, which is conducive to reducing the hull resistance.

There are also obvious differences in wave shapes of wake flow with different stern flaps. The variation of parameters such as length and cathedral angle directly affects the wave shape of wake flow field (Fig. 6). This indicates that as the stern flap length increases, the wake flow tends to lengthen, which to some extent determines the difference of the total resistance of hull with different stern flaps. Table 6 shows the resistance comparison of numerical simulation results with different stern flaps, in which R_t is the total resistance of numerical calculation.

Table 6 Resistance comparison of numerical simulation results with different stern flaps

Case	Fr=0.25		Fr=0.42	
	R_t/N	λ/%	R_t/N	λ/%
Bare body without stern flap	47.80	—	164.8	—
A	47.42	0.8	159.86	3.0
B	46.70	2.3	159.86	3.0
C	47.37	0.9	159.86	3.0
D	47.51	0.6	159.69	3.1
E	47.99	−0.4	159.20	3.4
F	47.70	0.2	159.53	3.2
G	47.75	0.1	159.03	3.5
H	47.94	−0.3	159.21	3.4
I	47.85	−0.1	159.04	3.5
J	48.09	−0.6	158.54	3.8
K	48.28	−1.0	159.20	3.4

The results of resistance calculation in Table 6 show that, after installing the stern flap, the hull resistance with stern flap is significantly reduced at the design speed (Fr = 0.42), and the resistance decrease rate is about 3%–4%. Moreover, the difference is small in the resistance reduction effect between different stern flaps. This shows that under this Froude number, the resistance reduction effect of the stern flap is obvious when the cathedral angle and length parameters are within a certain range, but the influence of the change in parameters on the resistance reduction effect of hull is not significant.

As can be seen from Table 6, compared with the design speed, the hull resistance varies greatly with different stern flap parameters at the cruise speed (Fr = 0.25). Among them, Case B has the most obvious effect, with a resistance decrease rate of about 2.3%. When the length and cathedral angle of stern flap increase to a certain extent, the hull resistance will increase to a certain degree.

4.3 Model test results and analysis

Based on the summary and analysis of the multi-scheme numerical simulation results and combined with the cruise speed and design speed, the optimization design goal of resistance reduction and efficiency increase at cruise speed and design speed is achieved and the test verification of multi-scheme stern flap model is carried out. The comparison of resistance decrease rates of model ship with different stern flaps is shown in Fig. 7. The delivered power $\frac{P_D}{\Delta}$ comparison of propeller per displacement of the ships without stern flap and with stern flap is shown in Fig. 8. Comparison of self-propulsion factors of the cases with stern flap and without stern flap is shown in Fig. 9. Where t is the thrust deduction; ω is the wake fraction; and V is the speed.

As can be seen from Fig. 7, under the design speed, five cases of fully-appended ship model with stern flaps have obvious resistance reduction effects. Compared with the case without stern flap, the resistance of the fully-appended ship model reduces by about 3%–4%, but the differences among different schemes are not obvious, which are consistent with the numerical simulation results. According to the self-propulsion test results shown in Fig. 8, the delivered power P_D of the propeller decreases by about 5%–6% compared with the case without stern flap. Fig. 9 shows that the thrust deduction t decreases and the wake fraction ω increases after stern flap is installed, which makes the hull efficiency η_H increases. However, the relative rotation efficiency η_R and the propeller efficiency η_0 have no obvious change. The total propulsion efficiency η_D increases by almost 2%. The difference of propulsion efficiency among different schemes is not obvious, which is the same as the law of resistance decrease.

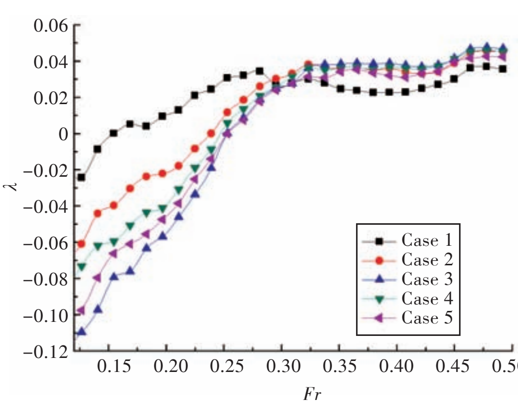

Fig.7 Comparison of model ship resistance decrease rate with different stern flaps

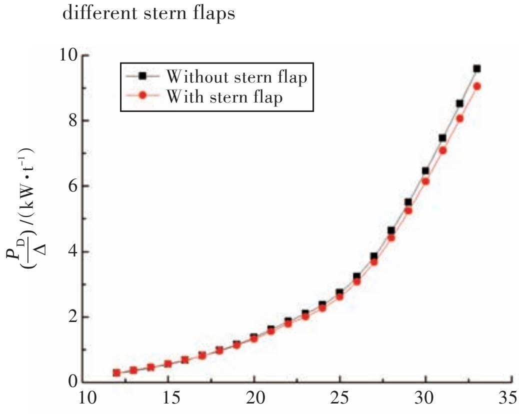

Fig.8 Delivered power comparison of propeller per displacement

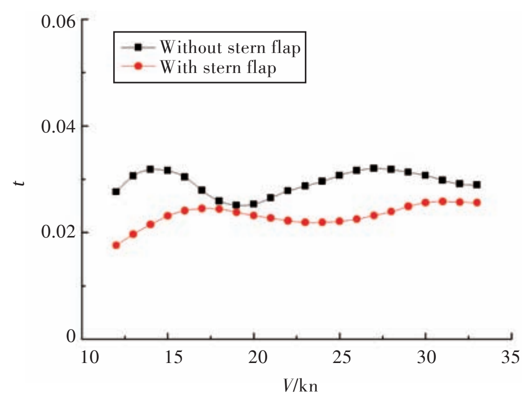

(a) Comparison of thrust deduction t

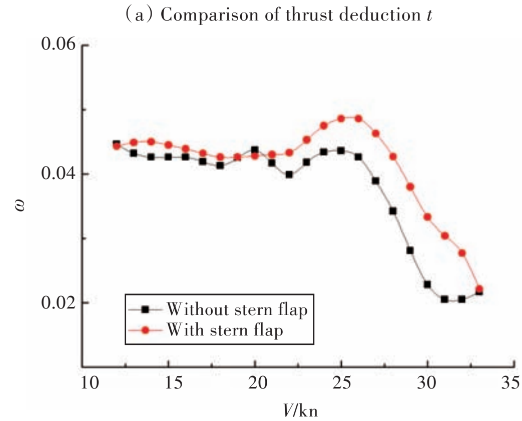

(b) Comparison of wake fraction ω

Fig.9 Comparison of self-propulsion factors

As can be seen from Fig. 7, there are certain differences in the resistance decrease effects of five stern flap cases at cruise speed. The resistance of Case 3, Case 4 and Case 5 is basically the same as that of the fully-appended ship model without stern flap. But the resistance decrease of Case 1 is about 3% and that of Case 2 is about 1%, which is consistent with the numerical simulation results. Fig. 8 shows that the change of the self-propulsion factors is not obvious, and therefore the change of the total propulsion efficiency η_D is also not obvious.

For the ship type and Froude number range, based on the comprehensive analysis of the resistance and self-propulsion test results of fully-appended ship models with and without stern flap, the following conclusions can be drawn.

1) The change of stern flap length and cathedral angle is sensitive to the influence of cruise speed, so the small stern flap length and cathedral angle can bring about resistance reduction effect in a cruise condition. If the design parameters, such as the length or the cathedral angle of stern flap are increased, the resistance reduction effect of cruise speed will be reduced, and when the parameters are increased to a certain extent, it will even increase the hull resistance.

2) At the design speed, the resistance reduction effect of installing stern flap is obvious. However, within a certain range of stern flap parameters, the influence of length and cathedral angle on resistance is not obvious. This shows that for this type of ship, the same resistance reduction effect can be obtained by the reasonable matching with different lengths and cathedral angles of stern flap within a certain range of stern flap parameters.

3) The influence of stern plate on the propulsion efficiency at cruise speed is not obvious, but it brings a certain increase to the propulsion efficiency at the design speed, especially the hull efficiency. But the influence of the change in parameters of stern flap on the propulsion efficiency is not significant.

5 Conclusions

In this paper, the numerical simulation calculation of viscous wave-making flow field, the resistance model test, and the self-propulsion model test are carried out for different stern flaps at cruise speed and design speed by the optimization design method combining multi-scheme numerical calculation and model test. The main conclusions are as follows.

1) By the numerical calculation method of the viscous wave-making flow field of displacement surface warship considering navigation attitude, the results of resistance prediction show that the error of resistance prediction and model test is within 5% at cruise speed and design speed, which meets the engineering accuracy. Moreover, the multi-scheme numerical calculation results are consistent with the results of model test, which can effectively guide the subsequent optimization design of stern flap.

2) Numerical simulation and model test results show that the selection of stern flap parameters is sensitive to the influence of rapidity at cruise speed. Therefore, for the future surface warships, the stealth design under cruise condition should be further strengthened, especially the follow-up stern flap design.

3) For this ship type, the results show that, by optimizing the stern flap parameters, energy consumption is reduced by 3% at cruise speed and 5% at design speed, and thus the goal of resistance reduction and energy saving at both cruise speed and maximum speed is achieved.

References

[1] Cheng M D, Liu X D, Wu C S, et al. Energy saving mechanism of stern flap installing on the high speed displacement ship [J]. Journal of Ship Mechanics, 2005, 9(2): 26-30 (in Chinese).

[2] Dong W C, Yao C B. Study on resistance prediction method and resistance reduction mechanism of medium & high speed deep-Vee ship by stern flap[J]. Journal of Harbin Engineering University, 2011, 32(7): 848-852 (in Chinese).

[3] Cheng M D, Liu X D, Zhang J W. Experimental study on effect of stern flap on power porforrmance of high speed surface warship[C]//The Collection of Academic Papers on Marine Hydrodynamics, [S.l.]: [s.n.], 2004 (in Chinese).

[4] Cheng M D, Liu X D, Yu J H, et al. Power performance investigation on a high-speed surface warships with a stern flap by sea trials[J]. Journal of Ship Mechanics, 2006, 10(2): 1-7 (in Chinese).

[5] Zheng Y, Dong W C, Yao C B. Experimental study on resistance reduction of displacement type deep-V hull model using stern flap[J]. Journal of Shanghai Jiaotong University, 2011, 45(4): 475-480 (in Chinese).

[6] Cusanelli D S. Scaling effects on stern flap performance, progress report[R]. [S.l.]: NSWCCD, 2009: 11.

[7] Cumming D, Pallard R, Thornhill E, et al. Hydrodynamic design of a stern flap appendage for the halifax class frigates[C]//Proceedings of MARI TECH 2006. Halifax, Canada: [s.n.], 2006.

[8] Cusanelli D S, Karafiath G. Advances in stern flap design and application[C]//Proceedings of the 6th International Conference on Fast Sea Transportation. Southampton, UK: [s.n.], 2001.

[9] Karafiath G, Cusanelli D, Lin C W. Stern wedges and stern flaps for improved powering-U.S. navy experience [J]. SNAME Transactions, 1999(107): 67-99.

[10] Zhou X. Energy saving effect of the stern flap on warship[J]. Marine Energy Saving, 1995(4): 48-51 (in Chinese).

[11] Zhang D Y, Zhang Y. On the effect of stern plate upon resistance performance of the high-speed catamaran [J]. Ship & Ocean Engineering, 2016(6): 20-23 (in Chinese).

[12] Zhang Z R, Li B Q, Zhao F. The comparison of turbulence models applied to viscous ship flow computation [J]. Journal of Hydrodynamics (Ser. A), 2004, 19 (5): 637-642 (in Chinese).

[13] Xu J, Yu J, Huang S F, et al. Application of turbulence models to prediction of powering performace for ship [J]. Shipbuilding of China, 2011, 52 (Supp 1): 53-58 (in Chinese).

[14] Wang F J. CFD analysis—principle and application of CFD software [M]. Beijing: Qinghua University Press, 2004 (in Chinese).

[15] Zhang S S. CFD and its application—principle and application of CFD software [M]. Wuhan: Huazhong University of Science & Technology Press, 2011 (in Chinese).

排水型水面舰船尾板参数优化设计

周芃*，傅江妍

中国舰船研究设计中心，上海 201108

摘　要：[**目的**] 尾板设计一般追求高速减阻，对于同时以巡航和设计航速为优化目标的水面舰船尾板设计，其航速覆盖范围广，需重点对尾板参数的选取予以研究。[**方法**] 采用计及航行姿态的粘性兴波流场数值模拟与模型试验验证相结合的设计方法，开展尾板多工况参数化优化设计。通过多方案数值仿真与阻力、自航模型试验的对比分析，总结得出尾板长度和下反角对于排水型水面舰船巡航和设计航速减阻节能的影响规律，并对CFD数值模拟结果的有效性进行初步的分析验证。[**结果**] 结果表明，通过对尾板参数的优化，巡航航速约可节能3%，设计航速约可节能5%，达到了巡航和最大航速同时实现减阻节能的设计目标。[**结论**] 所做研究可为后续排水型水面舰船尾板参数的优化设计提供理论支撑。

关键词：水面舰船；尾板；参数优化；数值模拟；模型试验

中图分类号：U662.2　　**文献标志码：**A　　**DOI：**10.19693/j.issn.1673-3185. 01370